AFRICAN WAVE DISTURBANCES IN A GENERAL CIRCULATION MODEL

M. A. Estoque, J. C. Jiing and J. Shukla

1983

Tellus

Volume 35A

Pages 287–295

Tellus (1983), *35A*, 287–295

African wave disturbances in a general circulation model

By M. A. ESTOQUE, J. SHUKLA[1] and J. G. JIING, *University of Miami, Rosentiel School of Marine and Atmospheric Science, 4600 Rickenbacker Causeway, Miami, Florida 33149, U.S.A.*

(Manuscript received July 5; in final form November 9, 1982)

ABSTRACT

Evidence is presented to show that African wave disturbances are reproduced in a general circulation simulation. The model used is the general circulation model developed by the Goddard Laboratory for Atmospheric Sciences of the National Aeronautics and Space Agency. The model was integrated in order to simulate the summer of 1974. A synoptic analysis of the simulated data over Africa for the month of July was done. The results of the analysis show that wave disturbances are generated by the model; the behavior and the structure of the simulated disturbances are similar to those observed over tropical Africa during the northern summer.

1. Introduction

The existence and the structure of synoptic scale disturbances over tropical North Africa have been studied observationally by numerous investigators, such as Carlson (1969a, b), Burpee (1974), and Reed et al. (1977). The disturbances occur primarily during the summer season and travel westward, sometimes developing into tropical cyclones over the Western Atlantic. The observational studies indicate that the disturbances usually have wavelengths of about 2500 km and propagation speeds of approximately 7° longitude per day. During the early summer the occurrence of disturbances is rather sporadic; they also tend to be weak in intensity. But later in the season they occur more or less regularly at intervals of about 4 days. However, even during this part of the summer, there are periods of relative inactivity, presumably due to unfavorable conditions in the large scale flow patterns in which the disturbances develop. Observational data indicate that the waves are most intense near the 700 mb level where the perturbations in the meridional wind component attain magnitudes of about 5 ms^{-1}. Reed et al. (1977) found that there is a secondary maximum near the 200 mb level with wind perturbations whose magnitudes are somewhat less than those of 700 mb. It may be mentioned that the relatively large wind perturbations at 200 mb are not reproduced satisfactorily by the theoretical models of Rennick (1976) and Mass (1979). This is possibly due to the fact that the primary mechanism for perturbation development in these models is barotropic instability; this may not actually be the case in the real atmosphere.

Some of the observed characteristics of the wind field associated with these disturbances are shown in Fig. 1. This is a series of four 24-hourly streamline maps at the 10,000 ft. level (approximately 800 mb) based on a previous study by Carlson (1969a). Note the general westward movement of the disturbances. Note also the development of Disturbance, W-4, between 10°E and 15°E and the weakening of Disturbance W-1 as it approaches the western coast of Africa. According to Carlson (1969b), the disturbances usually achieve their greatest intensity in the area between 10°W and 20°W; thereafter, they tend to disintegrate and to become disorganized.

The problem concerning the place of origin of these disturbances has been considered by several investigators. In his analysis of 1968 synoptic data,

[1] NASA, Goddard Space Flight Center, Greenbelt, Maryland.

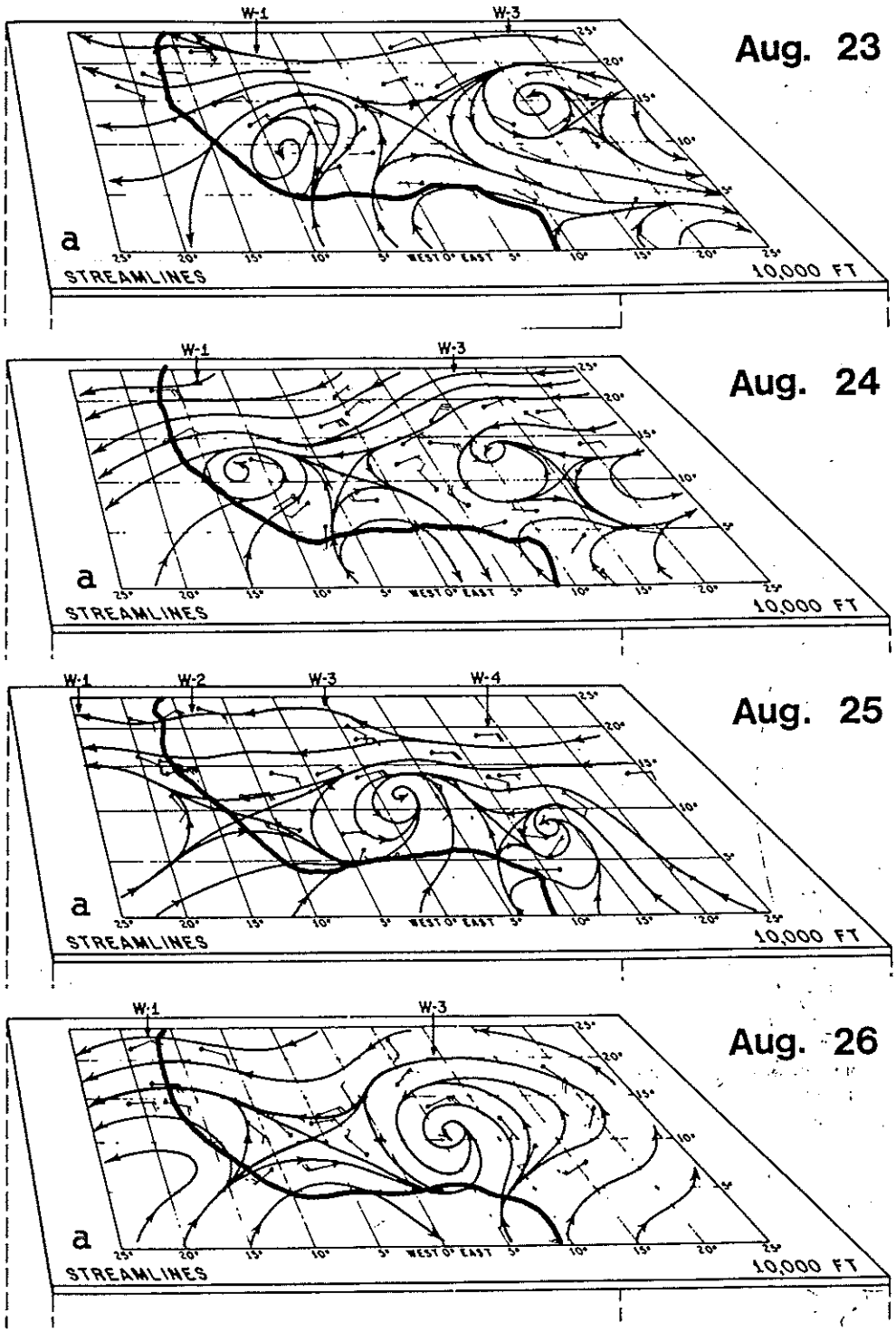

Fig. 1. Daily streamline maps at 10,000 ft (approximately 800 mb) during the period, August 23–26, 1967, based on Carlson's (1969a) synoptic analysis.

Carlson (1969b) showed that almost one half of the observed disturbances appeared to originate east of 18°E and only a few were first observed west of 4°E. The frequency distribution of initial wave positions has a minor peak between 10°E and 12°E. Burpee (1972) indicated that the disturbances form in the region between 15°E and 30°E. He found no clear evidence of waves at locations farther east at Khartoum (32°E) and at Aden (45°E). Subsequently, Dean and La Seur (1974) found that some disturbances originate near Khartoum. The finding that disturbances may originate farther east appears to be supported by the investigations of Aspliden (1974) as well as by Albignat and Reed (1980). In particular, the work of Albignat and Reed (1980) indicates that some disturbances may originate as far east as the southern tip of the Red Sea.

In regard to physical mechanisms which are responsible for the development of the disturbances, the observational study by Burpee (1972) as well as the theoretical studies by Rennick (1976) and by Mass (1979) suggest that barotropic instability is the major mechanism. However, on the basis of GATE observations, Norquist et al. (1976) found that baroclinic instability appears to be more important than barotropic instability over Africa. This finding is in agreement with a theoretical study of the energetics of the disturbances by Walker and Rowntree (1977) who concluded that barotropic instability made only minor contributions to the energy budget. A somewhat different generating mechanism has been suggested by Carlson (1969b). He suggests that the mechanism is associated with an interaction of the convective processes with the mountainous terrain over Cameroon as well as over Sudan and Ethiopia. Based on the above studies, one may conclude, therefore, that there is still no complete agreement concerning the mechanism for the generation of African disturbances.

The problem concerning the behavior, structure and the development of African disturbances may be investigated theoretically by using model simulations of the general circulation of the atmosphere. In the present paper, we will describe the initial results of such an investigation using simulation data from the NASA Goddard Laboratory for Atmospheric Sciences (GLAS) general circulation model. The basic characteristics of the model have been described previously by Sommerville et al. (1974). A detailed description of the parameterization of cumulus convection which is important in the tropics has been presented by Helfland (1979). Our preliminary results indicate that the model is able to simulate many of the important properties of African disturbances.

2. Data and analysis procedure

The simulated meteorological data which were available for our study are the horizontal wind components (u and v), temperature (T) and specific humidity (q). Values of these variables are given at nine levels of the atmosphere and on a horizontal grid whose grid points are spaced 5° longitudinally and 4° latitudinally. The initial conditions used in the numerical integration are based on observed data from May 1, 1974. Starting with these initial conditions, we integrated the model in order to make a simulation for the entire summer of 1974. Since the raw simulation data were quite noisy, we applied a band pass filter in order to retain only the perturbations within the spectral band whose wave numbers range from 8 to 20 along a latitude circle. Over the tropics, this spectral band corresponds to wavelengths from about 2000 to 5000 km along the east–west direction. The filtered values were obtained by computing the amplitudes of the Fourier components along the longitudinal direction which correspond to the above wave numbers; perturbation values represent the sum of the contribution of these wave numbers. Additional smoothing of the data was done along the north–south direction by using a method described by Shapiro (1970).

3. Results

Some general ideas concerning the existence and the properties of the simulated disturbances may be seen in Figs. 2, 3 and 4. These are Hovmoeller diagrams for the perturbation in the meridional component of the wind (v') the temperature (T') and the specific humidity (q') for 18°N. The perturbations correspond to deviations from local time means computed for each grid point. The diagram for v' encompasses the whole globe and corresponds to the three-month period of June, July and August 1974. The diagrams for T' and q' are only for the month of July 1974. Regions with

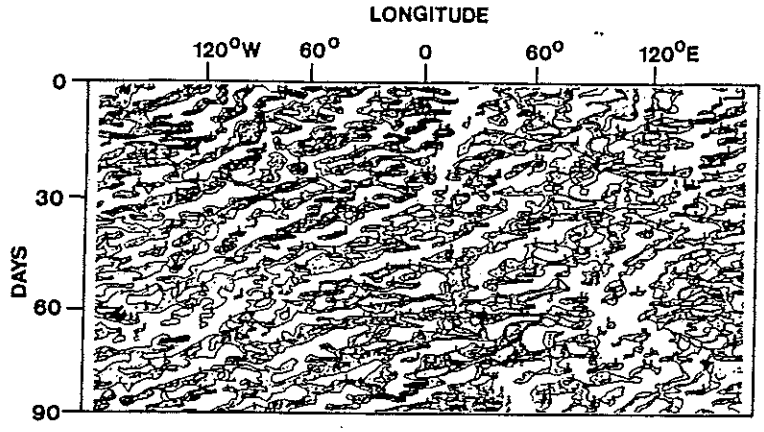

Fig. 2. Hovmoeller diagram for the perturbation north–south wind component along 18°N latitude during the period, June to August 1974, based on unfiltered simulation data. Areas with positive values are shaded.

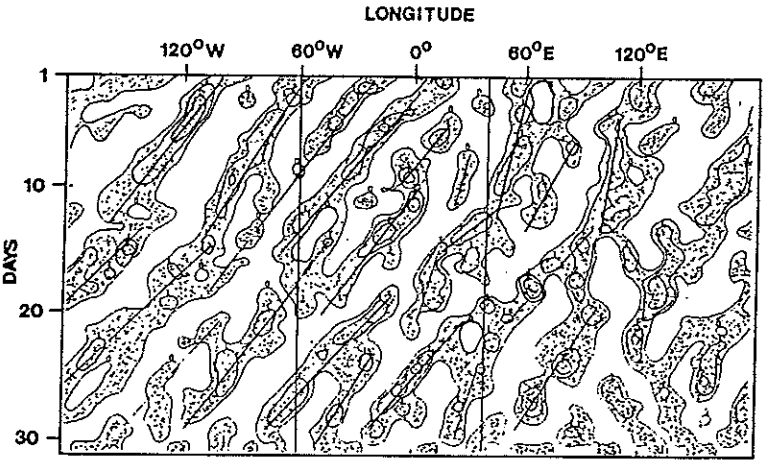

Fig. 3. Hovmoeller diagram for temperature perturbation along 18°N latitude during the month of July 1974 based on filtered simulation data. Areas with positive values are shaded. Contour interval in the shaded areas is 1 °C.

positive deviations are shaded. It may be seen that the patterns of shaded and unshaded areas in the diagrams demonstrate the existence of disturbances in the wind, temperature, and the moisture fields. The slope of the patterns from the lower left hand corner to the upper right corner near the Greenwich meridian imply a westward propagation of about 6 to 7 degrees of longitude, per day. This speed is close to that observed for African disturbances. Note that there is a general tendency for disturbances to develop over Central Africa (10°E) during the early part of July. The tendency is seen best in the Hovmoeller diagrams for v' and T'. However, later during the month, one can see evidence in these diagrams of disturbances which originate east of Africa.

More results relating to the development of disturbances over Africa are presented in Fig. 5, which shows the root mean square (RMS) of the perturbation v component and the mean wind vectors for July 1974 at 700 mb. It may be seen that there is a region of maximum values of the root mean square perturbation near the Greenwich meridian and 6°N. This region of large RMS of v'

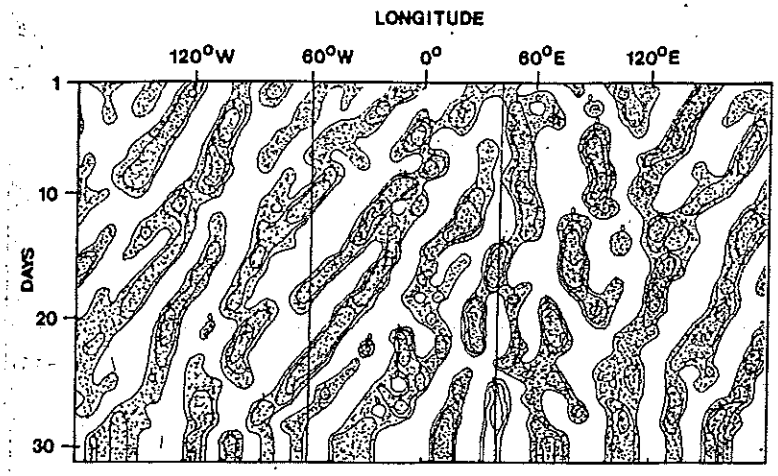

Fig. 4. Hovmoeller diagram for the specific humidity perturbation along 18°N latitude during the month of July 1974 based on filtered simulation data. Areas with positive values are shaded. Contour interval in shaded areas is 1 gram per kilogram.

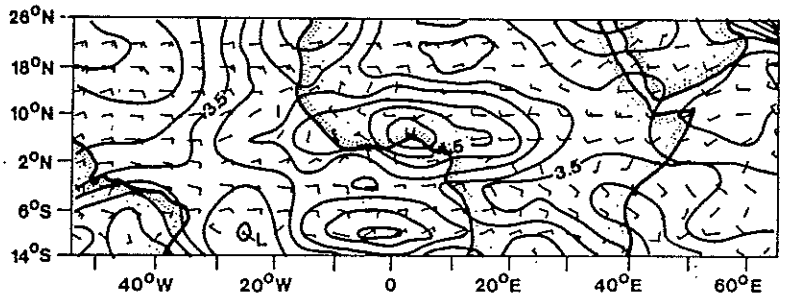

Fig. 5. Root mean square values of the perturbation in the meridional wind component and the mean wind at 700 mb for July 1974. The RMS values are in ms^{-1}; full barb for the wind vector corresponds to 5 ms^{-1}.

extends both eastwards and westwards but with decreasing values. Since the diagram is constructed using bandpassed data, the RMS values reflect only the contributions of disturbances with wavelengths from 2000 to 5000 km. The pattern of the isopleths indicates that the disturbances tend to intensify in the vicinity of 10°E. It is interesting to note that Carlson (1969b) found a relative maximum in the frequency distribution of initial wave positions in the same region. A similar region of intensification, although somewhat displaced westward, was found by Albignat and Reed (1980) by analysing GATE observations. The maximum value of the root mean square (4.5 ms^{-1}) is almost the same as the amplitude of the meridional wind oscillation in the 0.2 to 0.4 c.p.d. frequency band at 700 mb found by Albignat and Reed. In their analysis, Albignat and Reed also found a secondary maximum of wind oscillation amplitude just west of the Red Sea. Fig. 5 does not show a separate maximum in the same area; however, it may be noted that the region just southwest of the Red Sea is a region of large magnitudes of the root mean square v' relative to the regions located north and south. Fig. 5 also shows that disturbances tend to weaken west of the Greenwich meridian.

In order to illustrate the actual development of individual disturbances in the model simulations, we present a series of five 24-hourly maps in Figs. 6 to 10. The maps are streamline maps based on the

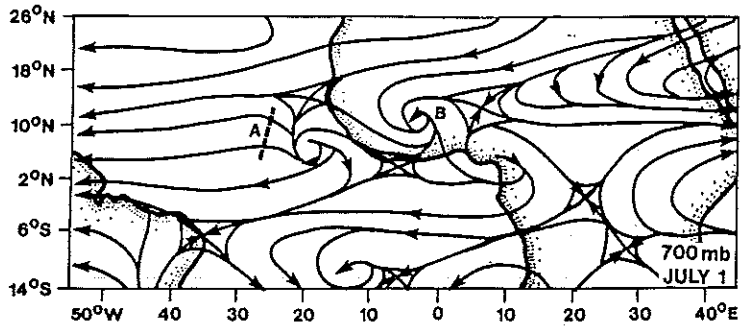

Fig. 6. Streamline map at 700 mb for 12Z July 1, 1974.

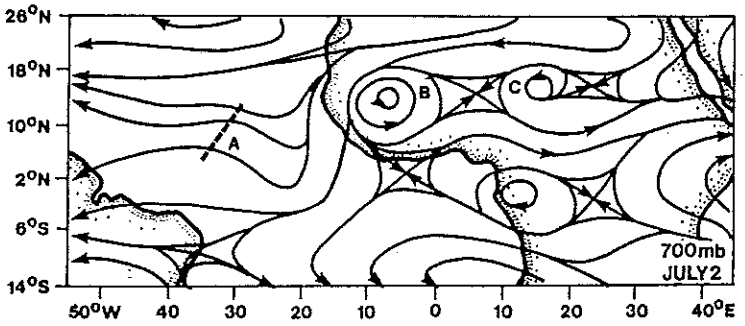

Fig. 7. Streamline map at 700 mb for 12Z July 2, 1974.

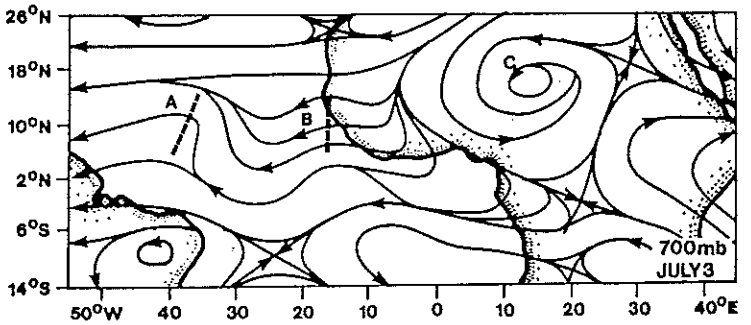

Fig. 8. Streamline map at 700 mb for 12Z July 3, 1974.

simulated 700 mb winds at gridpoints for the first 5 days of July 1974. Looking at the first map (12Z July 1, 1974), one can see two disturbances: a weak wave disturbance designated as A west of the West African Coast and a cyclonic vortex designated as B over West Africa near 10°N. In addition to these two synoptic features of the wind field, we also note a trough whose axis is oriented along the east–west direction, extending from Lake Chad (14°E, 14°N) to the Red Sea. During the next 24-hour period, wave disturbance A moves westward while the cyclonic vortex (B), intensifies and travels towards the west. At the same time, a cyclonic vortex (designated by C) forms at the western end of the east–west trough near Lake Chad (Fig. 7). The next two maps show further westward movement of the wave disturbance A. In the meantime, the cyclonic vortex B moves to the coast while

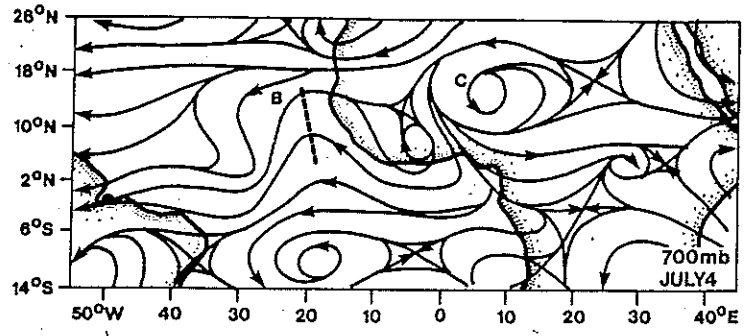

Fig. 9. Streamline map at 700 mb for 12Z July 4, 1974.

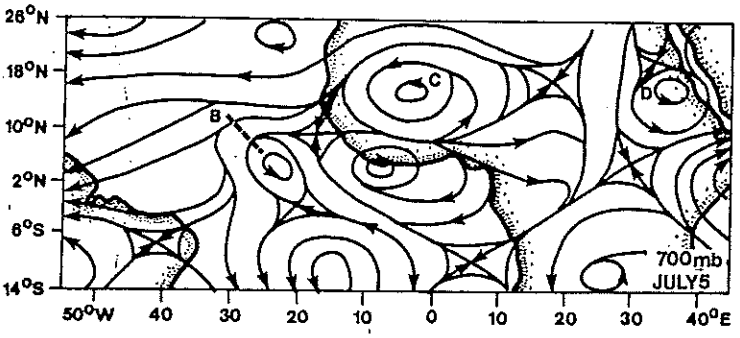

Fig. 10. Streamline map at 700 mb for 12Z July 5, 1974.

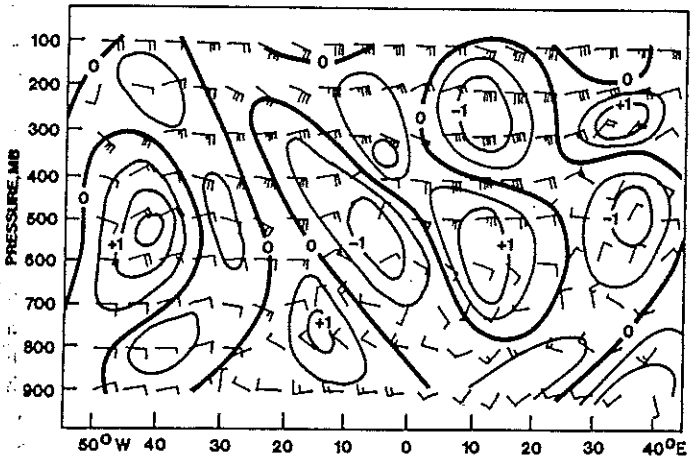

Fig. 11. Vertical cross section along 14 °N latitude for 12Z July 5, 1974. Isopleths represent isotherms of temperature deviations in °C; contour intervals are 0.5 °C. Wind barbs are total horizontal wind components; full barb is equal to 5 ms^{-1}.

decreasing in intensity and becoming just a trough. The cyclone near Lake Chad (C) intensifies and moves slowly westward. Finally, on the last map (12Z July 5, 1974), we see a new synoptic feature—a new cyclonic disturbance (D) which formed near the southern tip of the Red Sea. It is interesting to note that many features of the simulated 700 mb streamline maps resemble those of the observed streamline maps in Fig. 1.

In order to depict some of the important variations of the structure along the vertical direction, we have constructed Fig. 11. This diagram represents an east–west vertical section (at 14°N latitude) of the total wind and the temperature deviation at 12Z July 5, 1974; the 700 mb map which corresponds to this time is shown in Fig. 10. The latitude, which has been selected, runs close to the centers of the cyclonic vortices (C and D in Fig. 10) over Western Africa and near the Red Sea. The picture as a whole, shows a series of perturbations in the temperature and in the wind fields along the east–west direction. Maximum values of the temperature perturbations of about 1.5 °C are located near the 600 mb level. A secondary maximum appears close to the 300 mb level. The perturbations are small at 900 mb. Note that, in general, the troughs in the middle troposphere (near 30°W, 5°W, 35°E) are characterized by negative temperature deviations. The alternation of positive and negative temperature deviations at 600 mb along the east–west direction indicates an average horizontal wavelength of about 3500 km. Focusing our attention on the region (near 5°W) of the West African vortex (C), we see that this vortex is cold-cored near 600 mb. Above this cold core, the disturbance is warm-cored at the 300 mb level, i.e. the temperature variation at 300 mb is opposite in phase to that at 600 mb. This type of phase relationship seems to be characteristic of the entire region. There also appears to be a westward tilt with height of the patterns of isotherms. In regard to the wind field, one can see that the trough at 700 mb is overlaid by a weak ridge at 200 mb. This means that the southerly winds east of the 700 mb trough are overlaid by northerly winds at the 200 mb, i.e. an out-of-phase relationship in the v component at these two levels. An analogous phase relationship occurs west of the 700 mb trough. It is interesting to note that this vertical structure of the simulated disturbances is generally in agreement with that obtained by Reed et al. (1977) from GATE observational data.

4. Concluding remarks

In this paper we presented the results of a synoptic analysis of simulated data of the atmosphere over Africa and vicinity for the month of July 1974. The simulations were made by integrating the GLAS general circulation model for an entire summer season. The primary object of the analysis was to determine the existence, behavior, and the structure of synoptic scale disturbances over tropical Africa north of the equator. We found that the GLAS general circulation model is able to simulate rather realistically the observed characteristics of African disturbances. Some of the important characteristics of the simulated disturbances are as follows:

(1) During the month of July 1974, the disturbances intensify primarily in the region just south of Lake Chad and dissipate near the western coast of Africa. There is some indication that this intensification represents further development of already existing disturbances which have moved westward from the Red Sea region and in other regions even farther east.

(2) The disturbances have an average propagation speed of about 6° of longitude per day; the average horizontal wavelength is about 3000 km.

(3) The disturbances have a maximum amplitude near 600 mb; there appears to be a secondary maximum near the 300 mb level. The amplitude of the disturbance at 900 mb is relatively small.

(4) The troughs at 700 mb are characterized by negative temperature deviations. The temperature variations at 300 mb are out of phase relative to the variations at 700 mb. A similar out-of-phase relationship exists in the north–south wind component.

By and large, the above simulated characteristics are similar to those which have been found by analysis of observational data. In particular, the structure of the simulated disturbance is similar to that found by Reed et al. (1977) over continental Africa. The similarity between observed and simulated structure may indicate a corresponding similarity in the energetics, i.e. baroclinic processes may be more important than

barotropic processes over continental Africa. The agreement between simulated and observed disturbances may also indicate that these disturbances can be predicted eventually by numerical models of the type used in the present simulation.

5. Acknowledgements

This research was supported by the National Aeronautics and Space Administration under Grant No. NSG5342.

REFERENCES

Albignat, J. P. and Reed, R. J. 1980. The origin of African wave disturbances during Phase II of GATE. *J. Atmos. Sci. 37*, 1827–1839.

Aspliden, C. J. 1974. The low level windfield and associated perturbations over tropical Africa during northern summer. *Preprints Int. Tropical Meteorology Meeting*, Nairobi. Amer. Meteorol. Soc. 218–223.

Burpee, R. W. 1972. The origin and structure of easterly waves in the lower troposphere of North Africa. *J. Atmos. Sci. 29*, 77–90.

Burpee, R. W. 1974. Characteristics of North African easterly waves during the summers of 1968 and 1969. *J. Atmos. Sci. 31*, 1556–1570.

Carlson, T. N. 1969a. Synoptic histories of three African disturbances that developed into Atlantic hurricanes. *Mon. Wea. Rev. 97*, 256–276

Carlson, T. N. 1969b. Some remarks on African disturbances and their progress over the tropical Atlantic. *Mon. Wea. Rev. 97*, 716–726.

Dean, G. A. and LaSeur, N. E. 1974. The mean structure and the synoptic-scale variation of the African troposphere. *Preprints Int. Tropical Meteorology Meeting*, Nairobi, Amer. Meteorol. Soc., 224–228.

Helfland, H. M. 1979. The effect of cumulus friction on the simulation of the January Hadley Circulation by the GLAS model of the general circulation. *J. Atmos. Sci. 36*, 1827–1843.

Mass, C. 1979. A linear primitive equation model of African wave disturbances. *J. Atmos. Sci. 36*, 2075–2092.

Norquist, D. C., Recker, E. E. and Reed, R. J. 1977. The energetics of African wave disturbances as observed during Phase III of GATE. *Mon. Wea. Rev. 105*, 334–342.

Reed, R. J., Norquist, D. C. and Recker, E. E. 1977. The structure and properties of African wave disturbances as observed during Phase III of GATE. *Mon. Wea. Rev. 105*, 317–333.

Rennick, M. A. 1976. The generation of African waves. *J. Atmos. Sci. 33*, 1955–1969.

Shapiro, R. 1975. Linear filtering. *Math Comp. 29*, 1094–1097.

Sommerville, R. C., Stone, P. H., Halem, M., Hansen, J. E., Hogan, J. S., Druyan, L. M., Russel, G., Lacis, A., Quirk, W. and Tenenbaum, J. 1974. The GISS model of the global atmosphere. *J. Atmos. Sci. 31*, 84–117.

Walker, J. and Rowntree, P. R. 1977. The effect of soil moisture on circulation and rainfall in a tropical model. *Q. J. R. Meteorol. Soc. 103*, 29–46.